

**UNIVERSITY OF KALYANI**

**6th semester Dissertation**

SEW NARAYAN RAMESWAR

FATEPURIA COLLEGE



**NAME: ABDUR RAFIK SK**

**DEPARTMENT: PHYSICS HONS.**

**Subject :** ANALYSIS OF XRD, DSC AND  
ELECTRICAL  
DATA OF ZnO NANOPARTICLES DOPED  
PEO-LiI NANOCOMPOSITE ELECTROLYTE

**ROLL: 2116245 NO: 2075643**

**REG. NO.: 075381**

**SESSION: 2020-2021**

# ANALYSIS OF XRD, DSC AND ELECTRICAL DATA OF ZnO NANOPARTICLES DOPED PEO-LiI NANOCOMPOSITE ELECTROLYTE

A PROJECT WORK SUBMITTED FOR THE PARTIAL  
FULFILLMENT OF THE DEGREE OF MASTERS OF SCIENCE

IN

physics

By



*ABDUR RAFIK SK*

DEPARTMENT OF PHYSICS

UNIVERSITY OF KALYANI



sewnarayan Rameshwar Fatepuria college

***Table of content:***

1. Abstract
2. Introduction
3. Polymer Electrolyte
4. Aim Of the Project
5. Experimental technique
6. Result and Analysis
7. Conclusion & suggestion
8. Bibliography
9. Acknowledgement

NAME OF THE COLLEGE / INSTITUTION : S.R.FATEPURIA COLLEGE  
Address with pin code: S.R.F College Road ,Beldanga, PIN : 742133

Department of Physics

### CERTIFICATE

Certified that the Dissertation/ Project Work entitled **Analysis of XRD, DSC & Electrical data of ZnO Nanoparticle doped PEO-Lil Nanocomposite Electrolyte** carried out by

**ABDUL RAFIK SK.**, Registration No.075381 Year : **2020-2021**

and Roll : **2116245** No : 2075643, during the Academic session: **2020-2021** partial fulfilment for the award of BSc Physics

(Honours) Degree of University of Kalyani, Kalyani. The REPORT has been approved as it satisfies the academic

requirements in respect of Dissertation/ Project Work prescribed for the said Degree.

*Suman Mandal*

SIGNATURE OF THE GUIDE: 22-06-2023

SIGNATURE OF THE HOD: *[Signature]*

## DECLARATION

I hereby declare that the Dissertation/ Project work entitled

**Analysis of XRD, DSC & Electrical data of ZnO Nanoparticle doped PEO-LiI Nanocomposite Electrolyte** presented in this REPORT is my own work and has

been carried out during the Academic session 2020-2021, under the supervision of

**Mr. SUMAN MONDAL**, SACT, Department of

Physics, S.R. Fatepuria College in partial fulfilment for the award of BSc (Honors) Degree of

University of Kalyani, Kalyani and, that the REPORT has been prepared by me.

Further, I solemnly declare that, to the best of my knowledge, neither the whole nor a part of this REPORT

has been previously submitted to any University for any examination.

Abdul Rafik SK  
(Signature of student) 22/06/23

Date: Name of student: **ABDUL RAFIK SK**

Place: 6th semester BSc Physics (Honours)

Registration No **075381** Year: **2020-2021**

Roll : **2116245** No: **2075643**

**ABSTRACT** The demand of solid Polymer Electrolytes has increased now a days, as it is contributing very much in electrochemical devices. Due to some special features such as high energy density, better cycle ability and safety measures, various SPEs such as poly Ethylene oxide lithium salt complexes have become very attractive. Here in this paper Polymer Electrolyte and its ion transfer mechanism have been elaborately discussed. The aim of the project is mainly to explore the physical properties of polymer nanocomposite electrolyte such as PEO-LiI and novel PEO-LiI embedded in ZnO and investigate its behavior in dc conductivity. Different kind of technique and tool such as X-Ray Powder Diffraction method, Differential scanning calorimetry has been used here. Different parameters such as dc conductivity, ac conductivity have been investigated and it has been plotted against various entities to observe its behavior. The temperature dependence of dc conductivity of ZnO doped electrolytes is well explained by Arrhenius relation. After the study inference has been about the properties of the SPEs.

## INTRODUCTION

There is a growing demand in developing suitable solid polymer electrolytes (SPEs) as they have attracted much attention in developing electrochemical devices such as rechargeable solid state lithium ion batteries, fuel cells, capacitors and several new applications including biocompatible devices<sup>1-3</sup>. Among various solid polymer electrolyte (PEO)-lithium salt (LiX, X = I, CF<sub>3</sub>SO<sub>3</sub>, ClO<sub>4</sub> etc.) complexes<sup>4,5</sup> are much more attractive as they can offer number of advantages in terms of their high energy density, better cycle ability and safety<sup>6</sup> to be used as electrolyte in solid state battery and the ionic conductivity is the key parameter of their performance.

Though PEO has better flexibility, good complexation properties, the conductivity below melting point of PEO is restricted due to high crystalline phase. It is well established<sup>4</sup> that at room temperature the nature of PEO is biphasic containing both crystalline and amorphous phases and the transport of Li<sup>+</sup> cation in the polymer matrix is related to the local relaxation and segmental motion of PEO chains. The charge transfer process occurs when PEO is in the amorphous phase. Generally, PEO tends to crystallize below its melting temperature (m.p. 60°C) and thus shows much higher crystalline phases near room temperature and the conductivity of these electrolytes is much lower than 10<sup>-4</sup> S cm<sup>-1</sup>, which restricts its application in rechargeable batteries.

Over the last few decades many efforts have been made to increase the conductivity of these polymer electrolytes. The dissociation degree of lithium salts is essential for achieving high ionic conductivity in polymer complexes. This can be obtained when lattice energy of the salts is low and the host polymer has high dielectric constant. Also the addition of various plasticizers, such as tetraethylene glycol (TEG), ethylene carbonate (EC), propylene carbonate (PC) etc. to the polymer matrix increases their conductivity considerably<sup>7-8</sup>. However, they suffer from several drawbacks such as decomposition, volatilization, reaction towards lithium metal electrode and also the deterioration of the mechanical properties. It is seen that the addition of ceramic nanoparticle like Al<sub>2</sub>O<sub>3</sub>, TiO<sub>2</sub> in PEO-LiClO<sub>4</sub> electrolyte<sup>9,10</sup> and inclusion of inorganic nanoparticles as fillers in the PEO-lithium salt based polymer electrolytes<sup>11,12</sup> improves the conductivity considerably.

### 1.1 POLYMER ELECTROLYTE:

A polymer is a large molecule made by stringing together smaller molecules. Some examples of polymers of interest for polymer electrolytes are shown in Fig. 1.1 which includes polyethylene oxide (PEO), polypropylene oxide (PPO) and polyethylene imine (PEI).

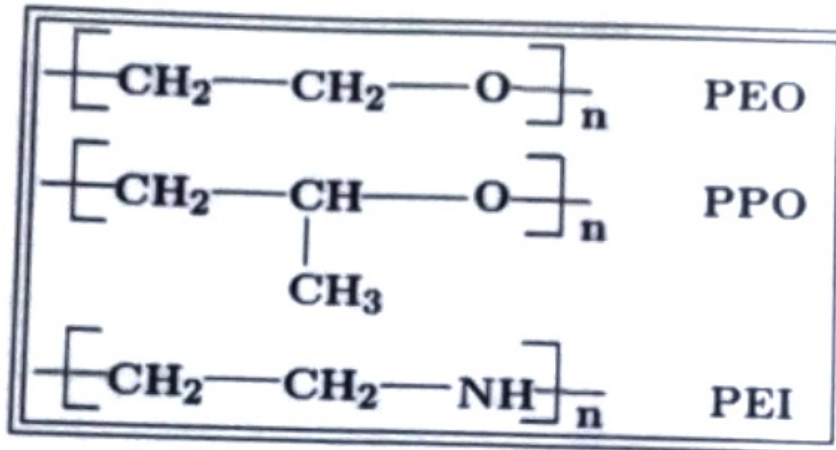


Fig 1.1: Some common polymers used for polymer electrolytes

A polymer electrolyte is formed by dissolving a salt into the polymer. Polymer electrolytes must function both as a separator and an electrolyte in solid-state rechargeable batteries. Polymer electrolytes should be rigid enough on a macroscopic level so that they can be used in the construction of all solid-state batteries and function as ion conductor and mechanical separator between the electrodes<sup>17</sup>. High molecular weight polymers are the suitable candidate as they have the ability to behave as a solid at a macroscopic level, while maintaining large segmental motions of chain backbones at temperatures above their glass transition temperature ( $T_g$ ). The physical entanglements, present in high molecular weight amorphous polymers, or the crystalline domains in semicrystalline polymers, prevent the material from flowing. Thus, these



materials may be classified as solids. It is because of this rubbery state that polymer electrolytes are attractive for battery applications.

### 1.2 ION TRANSPORT MECHANISM

Several studies<sup>18-20</sup> have been done on the ion transport mechanism in polymer electrolytes, but a clear picture of the movement of ion inside the polymer electrolyte is still lacking. During early investigations of these materials in the late 1970s, ion hopping through a rigid polymer framework, in which the cations were thought to move along channels within the

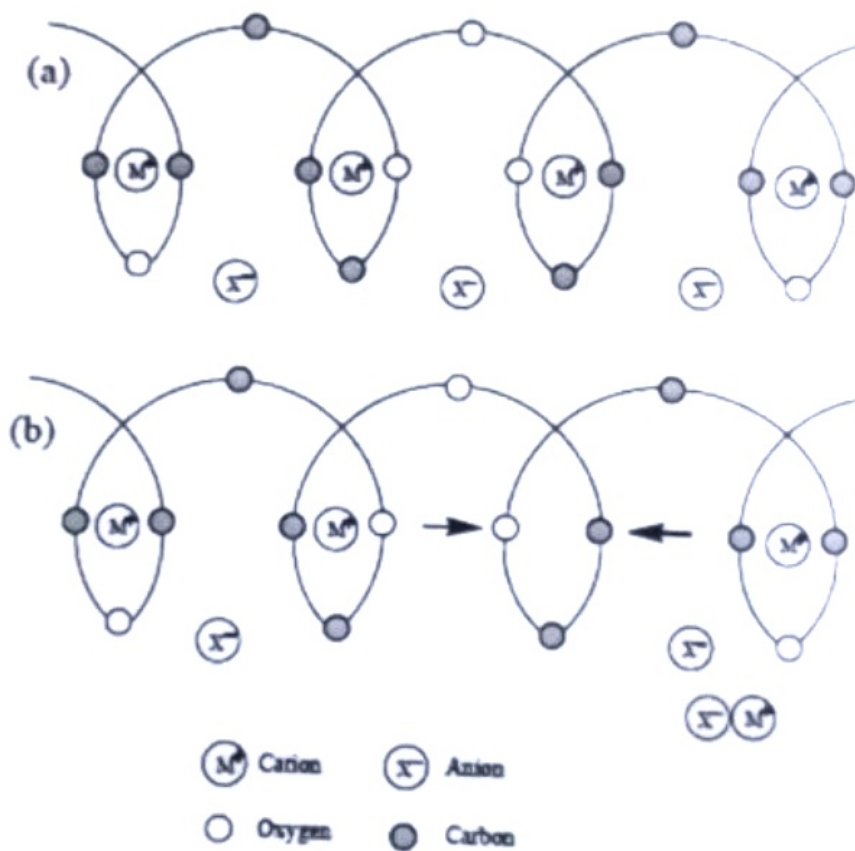


Figure 1.2: A helix model of the crystalline PEO/salt complex (a) Below  $T_m$  and (b) Above  $T_m$ .

PEO helices, was believed to be responsible for ion transport. Armand<sup>17</sup> suggested a helical structure with small ions lying inside the helix of PEO/salt complex as shown in Fig. 1.2. Assuming no anion motion, they proposed a hopping mechanism with only cations moving down channels within PEO helical crystalline structure.

This model cannot explain the ion motion in amorphous regions. The main distinction between ion transport in low-molecular-weight liquid electrolytes and in high-molecular-weight solid polymers electrolytes is that ion transport in the latter is decoupled from the macroscopic viscosity of the electrolytes. For polymer electrolytes, the polymer itself is the solvent and in a macroscopic sense the polymer solvent is immobile. This is because the polymer chains are

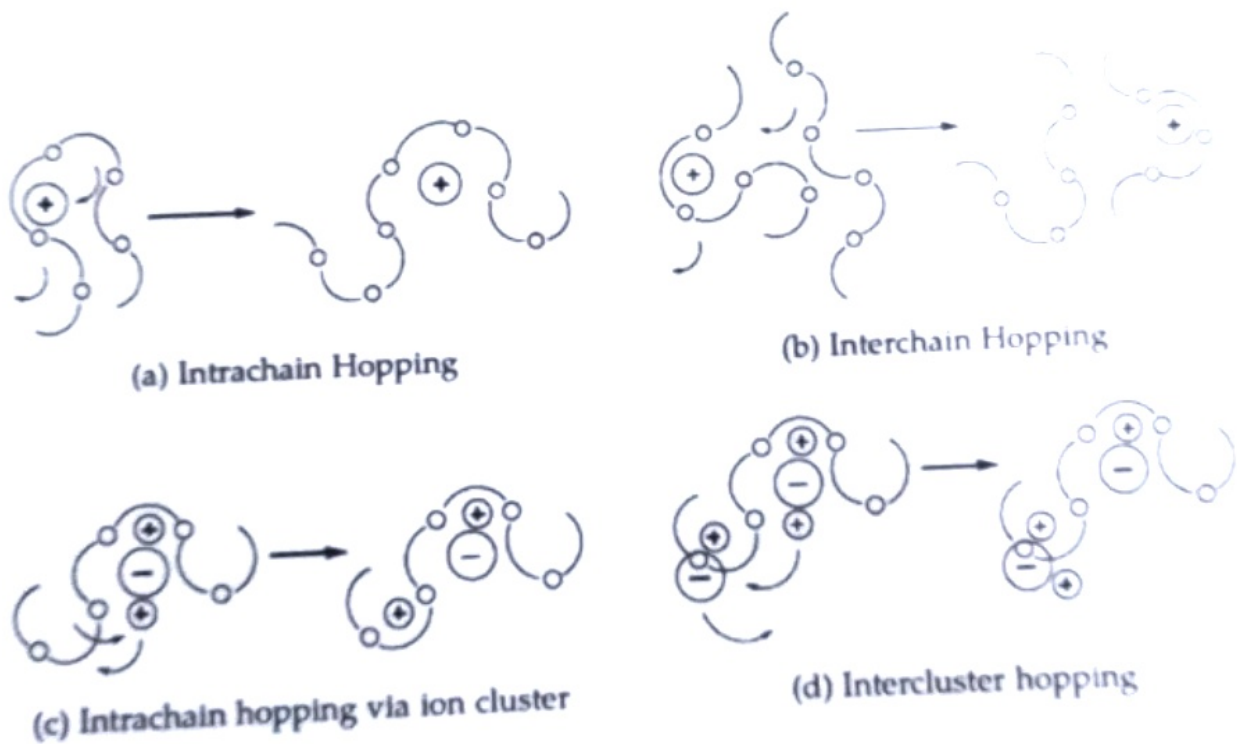


Figure 1.3: Schematic representation of segmental motion assisted lithium ion conduction mechanism in a host polymer matrix

entangled and cannot move over long distances with the ion. However, ion transport is intimately linked to the microscopic viscosity of short segments of the polymer chains. Polymer electrolytes can therefore be considered as extremely viscous fluids where the local motion of the polymeric solvent serves to transport the ions. Therefore, most of the research on new polymer electrolytes has been guided by the principle that ion transport is strongly dependent on local motion of the polymer in the vicinity of the ion. The segmental motions promote ion mobility through the formation and breaking of the co-ordinate bonds between the cations and host polymer, thus providing free volume in which the ions can diffuse/hop under the influence of an electric field.

Fig. 1.3(a) and Fig. 1.3(b) depict a cation motion through the coordinating sites of a single polymer chain and between sites of neighbouring chains. Fig. 1.3(c) and Fig. 1.3(d) shows movement of ions between ion clusters. As mentioned earlier in a semicrystalline polymer electrolyte the ion transport is predominant in the amorphous region. In these region polymer acquires faster internal modes where bond rotations produce segmental motion, which in turn facilitates ionic jumps between inter- and intra-chains, and the ionic conductivity of polymer electrolytes increases towards higher values.

### **1.3. AIM OF THE PROJECT:**

The raw data sets obtained for PEO-LiI electrolyte and PEO-LiI - 0.1 wt % ZnO nanocomposite electrolytes have been analyzed to explore the physical properties such as crystallinity, melting temperature, glass transition temperature. Also analyzing the electrical data sets, we tried to explore the effect of addition of ZnO nanoparticles in PEO-LiI electrolytes; whether it increases the dc conductivity of the sample or not. Different models have been used to extract the information from complex impedance spectra data sets and ac conductivity data sets. Also the temperature dependent profiles of the dc conductivity data of the samples have been fitted using different

functions and some valuable information have been achieved.

## 2. EXPERIMENTAL TECHNIQUE:

### 2.1. X-RAY POWDER DIFFRACTION :

X-ray powder diffraction (XRD) is a rapid analytical technique primarily used for phase identification of a crystalline material and can provide information on unit cell dimensions. The analyzed material is finely ground, homogenized, and average bulk composition is determined.

#### FUNDAMENTAL PRINCIPLE OF X-RAY POWDER DIFFRACTION:

Max von Laue, in 1912, discovered that crystalline substances act as three-dimensional diffraction gratings for X-ray wavelengths similar to the spacing of planes in a crystal lattice. X-ray diffraction is now a common technique for the study of crystal structures and atomic spacing.

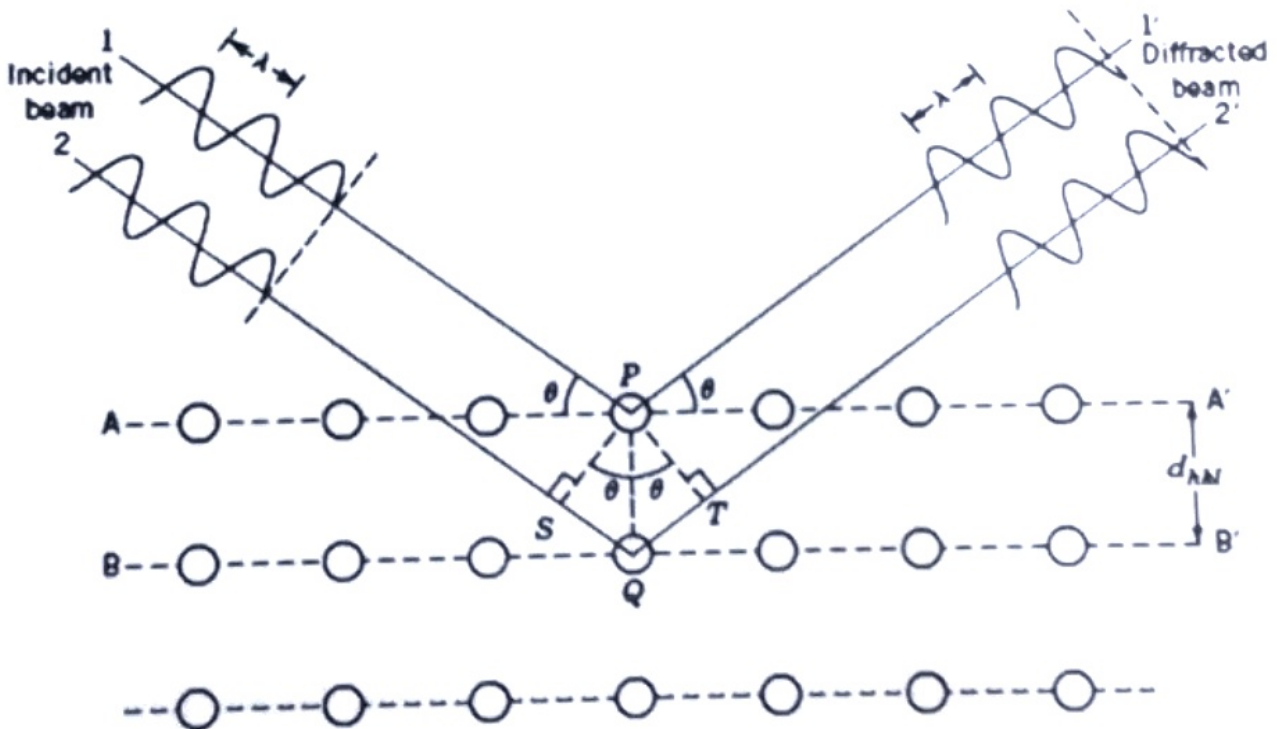


Figure 2.1: Visualization of the Bragg law

X-ray diffraction is based on constructive interference of monochromatic X-rays and a crystalline sample. These X-rays are generated by a cathode ray tube, filtered to produce monochromatic radiation, collimated to concentrate, and directed toward the sample. The interaction of the incident rays with the sample produces constructive interference (and a diffracted ray) when conditions satisfy Bragg's Law ( $n\lambda = 2d \sin \theta$ ). This law relates the wavelength of electromagnetic radiation to the diffraction angle and the lattice spacing in a crystalline sample. These diffracted X-rays are then detected, processed and counted. By scanning the sample through a range of  $2\theta$  angles, all possible diffraction directions of the lattice should be attained due to the random orientation of the powdered material. Conversion of the diffraction peaks to d-spacings allows identification of the mineral because each mineral has a set of unique d-spacings. Typically, this is achieved by comparison of d-spacings with standard reference patterns.

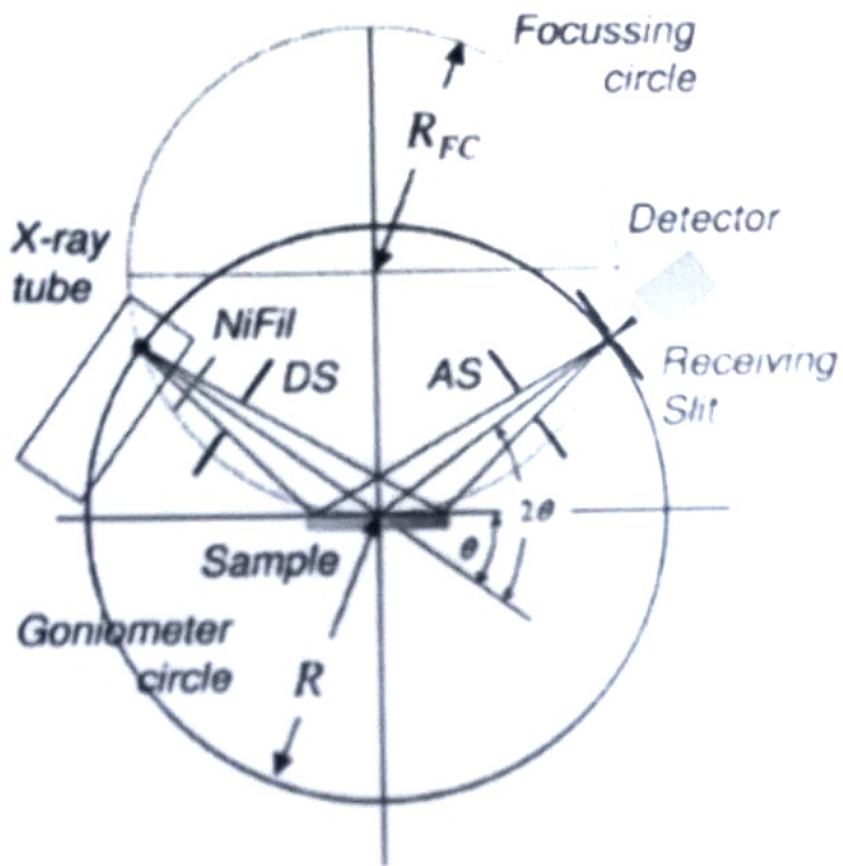


Figure 2.2: Schematic representation of  $\theta/2\theta$  diffraction in Bragg-Brentano geometry.

All diffraction methods are based on generation of X-ray in an X-ray tube. These X-rays are directed at the sample, and the diffracted rays are collected. A key component of all diffraction is the angle between the incident and diffracted rays.

Powder and single crystal diffraction vary in instrumentation beyond this.

The basic measurement geometry used in most of the x-ray diffraction instrument is depicted in Fig. 2.2. The sample should preferably exhibit a plane or flattened surface. The angle of both the incoming and the exiting beam is  $\theta$  with respect to the specimen surface. Its measurement geometry may also be applied to the investigation of thin films, especially if the layer is polycrystalline and has been deposited on a flat substrate, as is often the case. The diffraction pattern is collected by varying the incidence angle of the incoming x-ray beam by  $\theta$  and the scattering angle by  $2\theta$  while measuring the scattered intensity  $I(2\theta)$  as a function of the latter. Two angles have thus to be varied during a  $\theta/2\theta$  scan. In one case the x-ray source remains fixed while the sample is rotated around  $\theta$  and the detector moves by  $2\theta$ . In another case the sample is fixed while both the x-ray source and the detector rotate by  $\theta$  simultaneously, but clockwise and anticlockwise, respectively. The rotations are performed by a so-called goniometer, which is the central part of a diffractometer. Typically the sample is mounted on the rotational axis, while the detector and/or x-ray source move along the periphery, but both axes of rotations coincide.

## 2.2 DIFFERENTIAL SCANNING CALORIMETRY (DSC):

Differential scanning calorimetry (DSC) is an effective analytical tool for characterizing the physical properties of a polymer. DSC enables determination of melting crystallization, and mesomorphic transition temperature, and the corresponding temperature, enthalpy and entropy changes, and characterization of the glass transition and other effects which show either changes in heat capacity or a latent heat.

DSC has proven to be a very reliable technique to obtain heat capacity at elevated temperature in a reasonable short time. DSC also enables study of the kinetic transitions in a wide dynamic range. Because of its simplicity and ease of use, DSC is widely applied to polymer science.

Calorimetry is generally based on the following relationship:

$$\delta Q = C \cdot \Delta T = c \cdot m \cdot \Delta T$$

or, in differential form, assuming time independent sample mass and specific heat capacity:

$$\delta Q/dt = \Phi = C dT/dt = c m \beta$$

where  $\delta Q$  = the heat exchanged,

$\Delta T$  = the temperature change caused by the exchanged heat

$\Phi$  = the heat flow rate,

$C$  = the heat capacity,

$c = C/m$  is the specific heat capacity,

$m$  = the sample mass,

$\beta$  = the scan rate (heating or cooling)

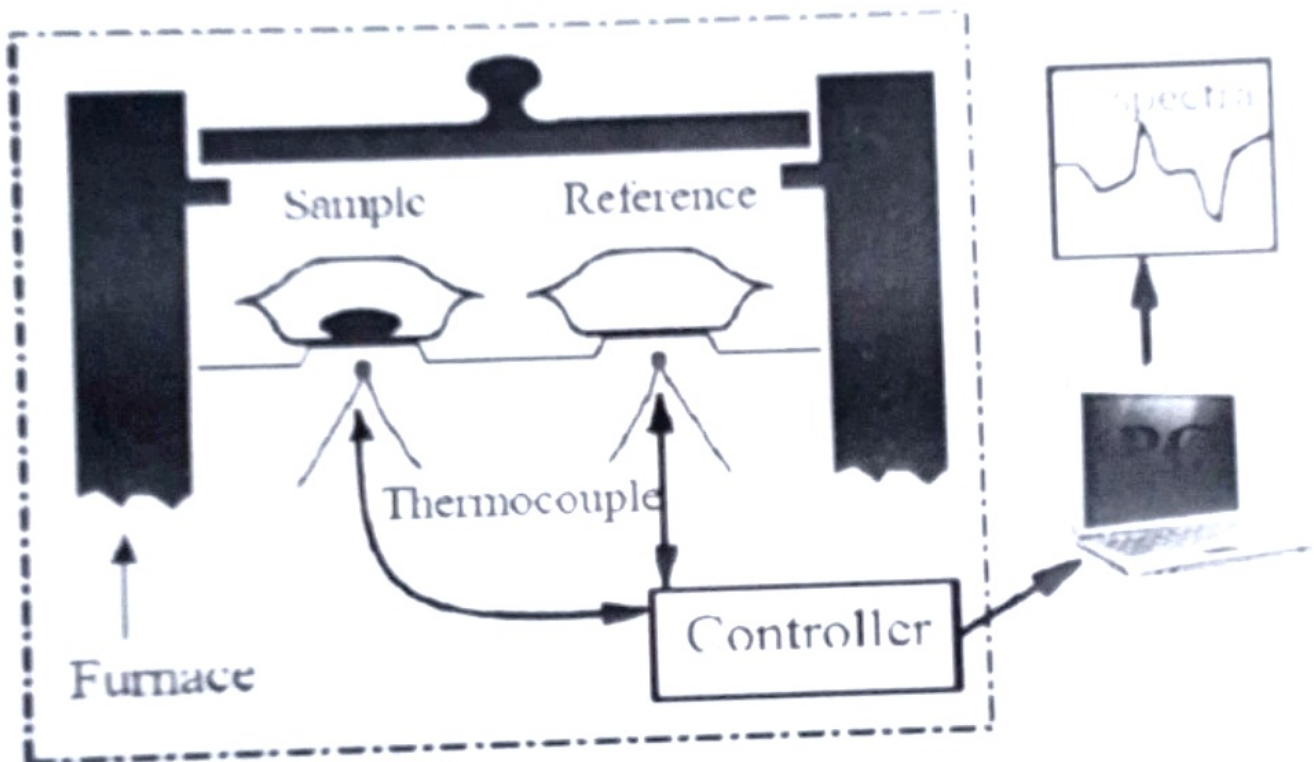


Figure 2.3: Schematic drawing of DSC measurement technique

Here we will mainly use the DSC to study the semi-crystalline polymers depending



on the mode of operation effects like melting, Crystallization and glass transition

### 3. ANALYSIS:

#### 3.1 X-RAY DIFFRACTION (XRD):

Two diffraction peaks (at  $2\theta = 19^\circ$  and  $23.5^\circ$ ) are observed for PEO-LiI electrolyte which are the characteristic peaks of PEO due to its crystalline phase. Fig 3.1 clearly indicates that the PEO-LiI electrolyte shows highest peak intensity, suggesting highest crystalline phase of PEO.

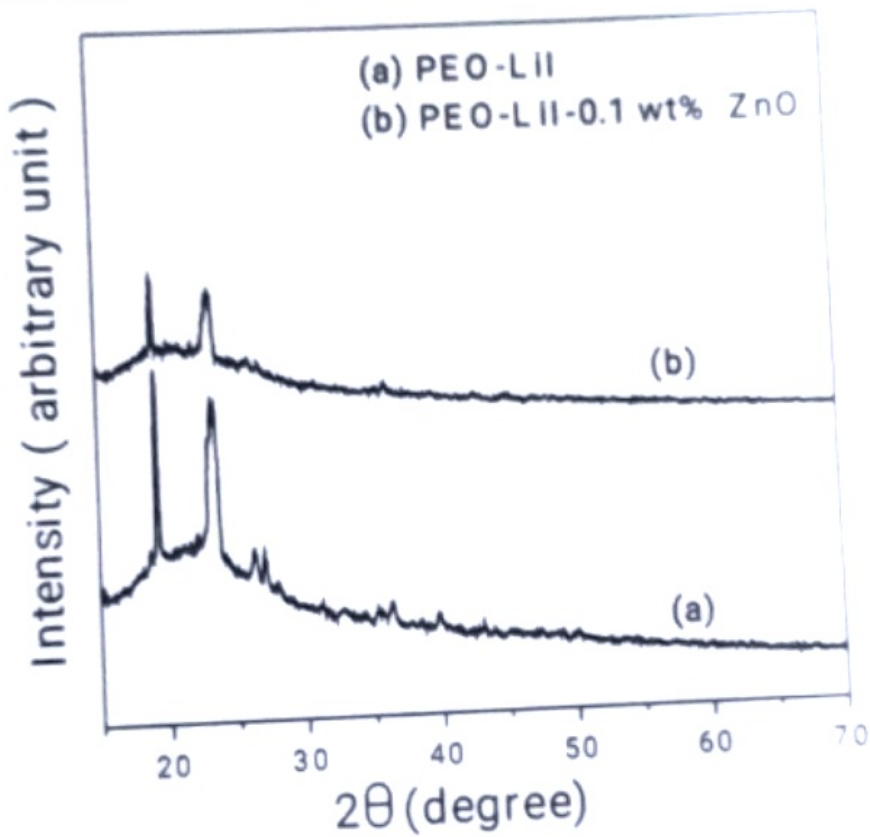


Fig 3.1: (a) X-ray diffraction pattern for PEO-LiI-0.1 wt% ZnO polymer electrolytes

(b) X-ray diffraction pattern for PEO-LiI polymer electrolytes.

With the addition of ZnO in the PEO-LiI matrix, the peak intensity of crystalline PEO decreases and only trace of crystalline PEO has been detected for 0.05 wt% ZnO nanoparticles in the PEO-LiI matrix, indicating that significant reduction in the crystalline phase of PEO and a homogeneous electrolyte with a high degree of dispersion of the ZnO occurs for this composition.

**3.2 DIFFERENTIAL SCANNING CALORIMETRY (DSC):**

The DSC traces of PEO-LiI and PEO-LiI -0.1 wt % ZnO nanocomposite electrolytes are displayed in Fig. 3.2. The thermodynamic parameters such as glass transition temperature ( $T_g$ ), melting temperature ( $T_m$ ), and melting enthalpy ( $\Delta H_m$ ) were obtained from the DSC traces and are summarized in Table 1. The percentage of crystalline phase of PEO ( $X_c$ ) has been calculated using the equation

$$X_c = \frac{\Delta H_m}{\Delta H_{PEO}} \quad (1)$$

where  $\Delta H_m$  is the melting enthalpy of the sample and  $\Delta H_{PEO}$  is the melting enthalpy (namely 213.7 J/g) of completely crystallized PEO.

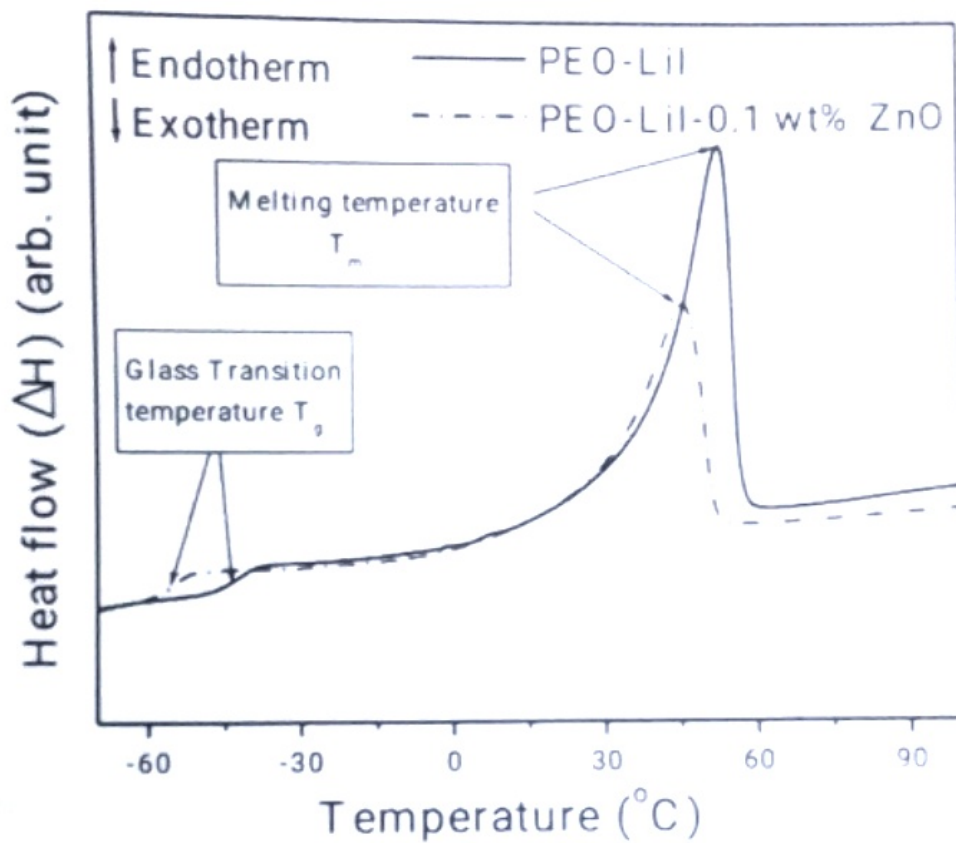


Fig 3.2: (a) DSC thermograph for PEO-LiI – 0.1 wt % ZnO polymer electrolytes

(b) DSC thermograph for PEO-LiI polymer electrolytes

For the calculation of  $\Delta H_m$ , the area under the melting peak has been determined using Origin 6.0 software with proper choosing of base line

**Table (1): Comparison of thermal parameters obtained from DSC and dc conductivity obtained from ac conductivity spectra for PEO-LiI and (b) PEO-LiI 0.1 wt % ZnO nanocomposite electrolytes.**

wt% ZnO	$T_g$ ( $^{\circ}\text{C}$ )	$T_m$ ( $^{\circ}\text{C}$ )	$\Delta H_m$ (J/g)	$X_c$ (%)	$\sigma_{dc}$ ( $\Omega^{-1}\text{cm}^{-1}$ ) T=293 K
0	-42	52	67.69	31.68	$1.4 \times 10^{-8}$
0.05	-55	45	50.35	23.56	$5.1 \times 10^{-7}$

It can be observed that when ZnO nanoparticles is doped into PEO-LiI polymer electrolyte the glass transition temperature  $T_g$  decreases from  $-42^{\circ}\text{C}$  to around  $-55^{\circ}\text{C}$  and also the melting temperature  $T_m$  decreases from  $52^{\circ}\text{C}$  to around  $45^{\circ}\text{C}$ . This result suggests the improvement in the flexibility of the polymer host backbone which in turn is expected to facilitate the segmental motion of PEO chain.

It is noted in Table 1 that the values of  $\Delta H_m$  decrease with the addition of ZnO nanoparticles in PEO-LiI electrolytes. A lower  $\Delta H_m$  value shows a reduced degree of crystalline phase. This decrease in crystallinity of PEO is due to the fact that the introduction of ZnO nanoparticles lowers the reorganization tendency of polymer chain via the interaction with  $\text{Li}^+$  and PEO, promoting more amorphous regions and leading to the formation of an amorphous interface area surrounding the nanoparticles.

### **3.3. ELECTRICAL CHARACTERIZATION:**

The most important parameter for the polymer electrolytes is its ionic conductivity or dc conductivity. The dc conductivity of the samples was determined in two ways

1. from the complex impedance plots and
2. from the extrapolation of the frequency dependent conductivity to zero frequency

For a particular temperature the real and imaginary parts of the complex impedance  $Z^* = Z' + Z''$  at frequency  $\omega$  were determined from the following relations

$$Z' = \frac{G(\omega)}{G^2(\omega) + \omega^2 (C(\omega) - C_0)^2} \quad (2)$$

$$Z'' = \frac{G(\omega)(C(\omega) - C_0)}{G^2(\omega) + \omega^2 (C(\omega) - C_0)^2} \quad (3)$$

where  $C_0$  is the capacitance of the sample cell without sample. In the polymer electrolyte field, the display of the so-called complex plane representation, in which  $Z''$  (y-axis) is plotted against  $Z'$  (x-axis), is much favored. This display is characterized for polymer electrolytes by arcs, which have the form of depressed or flattened semicircles, and straight lines, inclined to the x-axis, which are usually called tilted spikes. The advantages of this form of data presentation are that each arc or spike is characteristic of a particular region of the cell and that the bulk resistance can be easily computed from the plot.

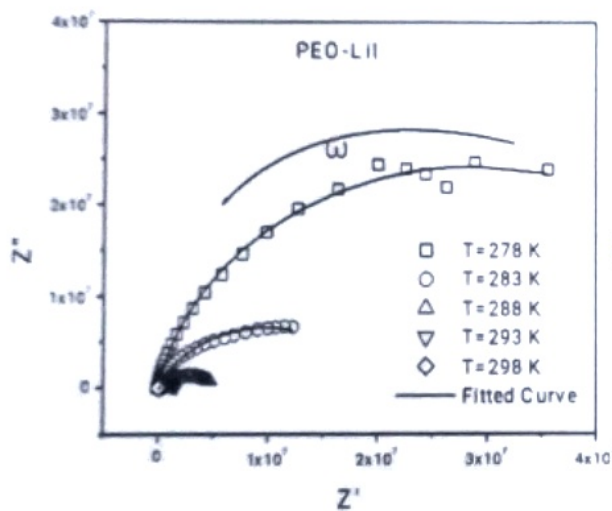


Fig 3.3: Complex impedance plots of PEO-LiI electrolyte at different temperatures

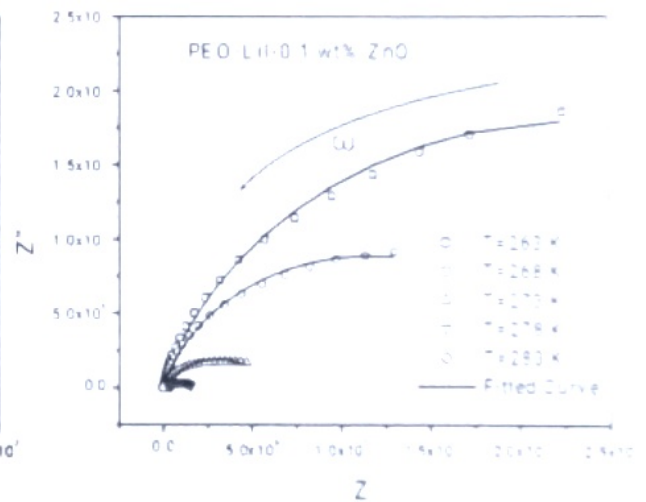


Fig 3.4: Complex impedance plots of PEO-LiI-0.1 wt% ZnO electrolyte at different temperatures

From the complex impedance plots, the dc resistance  $R$  was calculated at different temperatures and then dc conductivity was calculated using the relation

$$\sigma_{dc} = \frac{1}{R} \left( \frac{l}{A} \right) \quad (4)$$

Where  $l$  and  $A$  are the thickness and area of the sample respectively. Typical complex impedance plots for PEO-LiI and PEO-LiI-0.1 wt% ZnO electrolytes at different temperatures are shown in Fig. 3.3 and Fig. 3.4 respectively. It is clearly seen from the figure that the dc resistance  $R$  decreases with the increase of temperature. A comparison of the complex impedance plots for PEO-LiI and PEO-LiI-0.1 wt% ZnO electrolytes at  $T = 293$  K is shown in Fig. 3.5

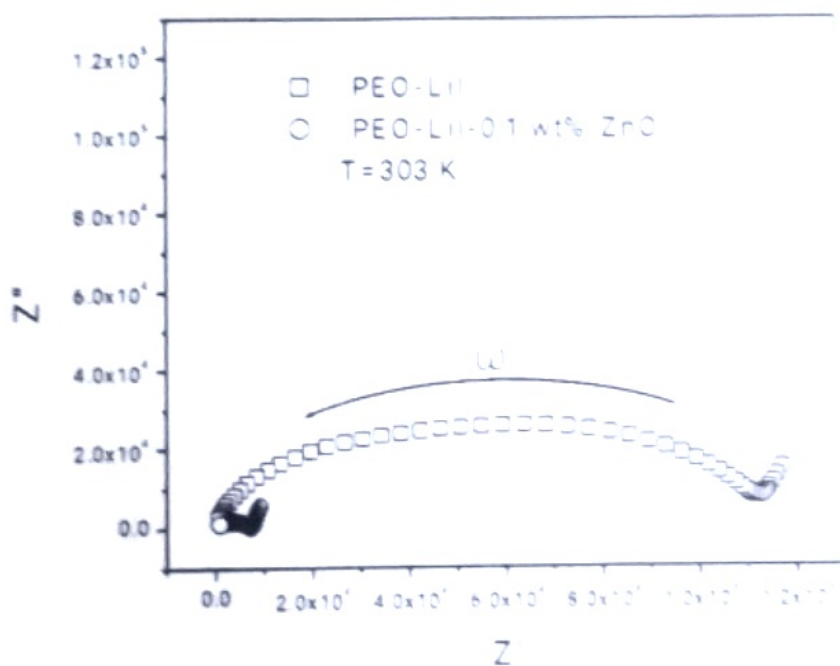


Fig. 3.5: Complex impedance plots of PEO-LiI and PEO-LiI-0.1 wt% ZnO electrolytes at a fixed temperature T=303 K.

At low frequencies inclined spikes are observed due to electrode/electrolyte polarization. It is observed that the dc resistance  $R$  is lower in PEO-LiI-0.1 wt% ZnO electrolyte compared with PEO-LiI electrolyte. The dc electrical conductivity obtained from the complex impedance plots for PEO-LiI and PEO-LiI-0.1 wt% ZnO electrolytes is shown in Fig. 3.6 as a function of reciprocal temperature. It is noted that the plots in all cases are straight line type and can be fitted to the Arrhenius relation

$$\sigma = \sigma_0 e^{-\frac{E_a}{k_B T}} \quad (5)$$

where,  $\sigma_0$  is the pre-exponential factor,  $E_a$  the activation energy,  $k_B$  the Boltzmann constant and T is the absolute temperature. The linearity of the  $\log \sigma$  versus  $1/T$  plots is consistent with ion hopping in a semicrystalline polymer electrolyte. The activation energy for the conduction process reflects an energy barrier for the ions to hop from one site to another in the polymer complex.

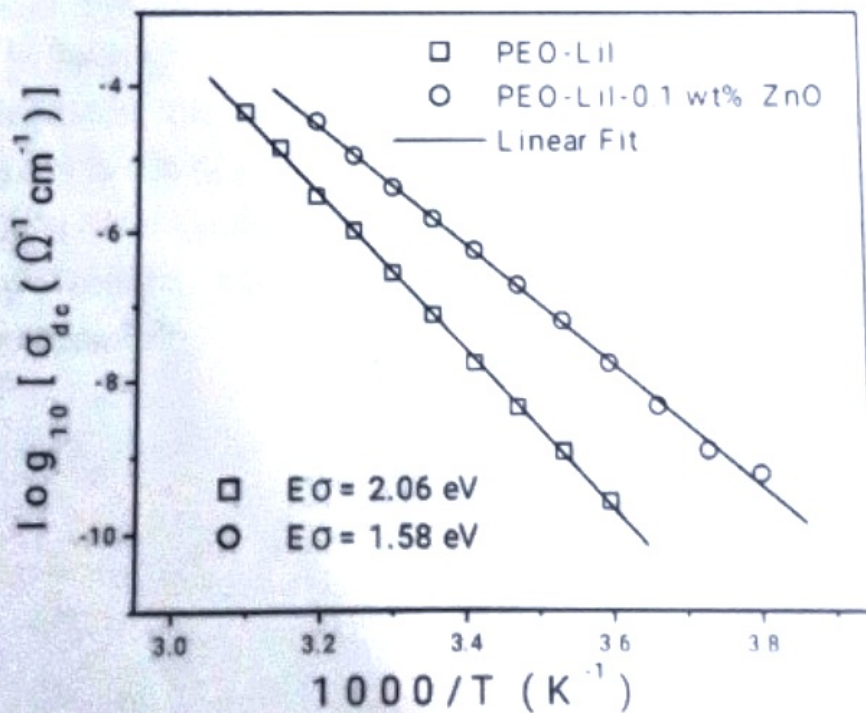


Fig. 3.6: Dc conductivity plotted as a function of inverse temperature for PEO-LiI and PEO-LiI-0.1 wt% ZnO electrolytes. The solid lines are the least square straight-line fits to the experimental data

This barrier is determined by the polymeric environment of the ions. When an ion hops from one coordination site to another, the originally occupied site relaxes and the new site deforms to accommodate the incoming ion. The values of  $E_a$  have been obtained from the least square straight line fits and are shown in the figure. The lower value of  $E_a$  indicates that the energy barrier is much lower in PEO-LiI-0.1 wt% ZnO electrolyte compared with PEO-LiI electrolyte which is much more favorable condition for ion conduction.

The frequency dependence of the ac conductivity at different temperatures is shown in Fig. 3.7 and Fig 3.8 for the PEO-LiI and PEO-LiI-0.1 wt % ZnO nanocomposite electrolytes, while Fig. 3.9 shows the same at 293 K for the two composites for a fixed temperature. The frequency dependent conductivity spectrum (Fig. 3.9) exhibits three distinguished regions. Due to polarization effects at the electrode-electrolyte interfaces the low frequency dispersion is observed. As the frequency reduces charge accumulation at the electrode-electrolyte interfaces takes place and drops the conductivity. In the intermediate frequency region conductivity is almost found to be frequency independent. The random diffusion of the ionic charge carriers via activated hopping gives rise to this type of frequency independent dc conductivity and are equal to dc conductivity  $\sigma_{dc}$  of the sample. At higher frequencies the time period available is short and the probability for the ions to go to another favorable site and fall back to their original site increases<sup>21,22</sup>.



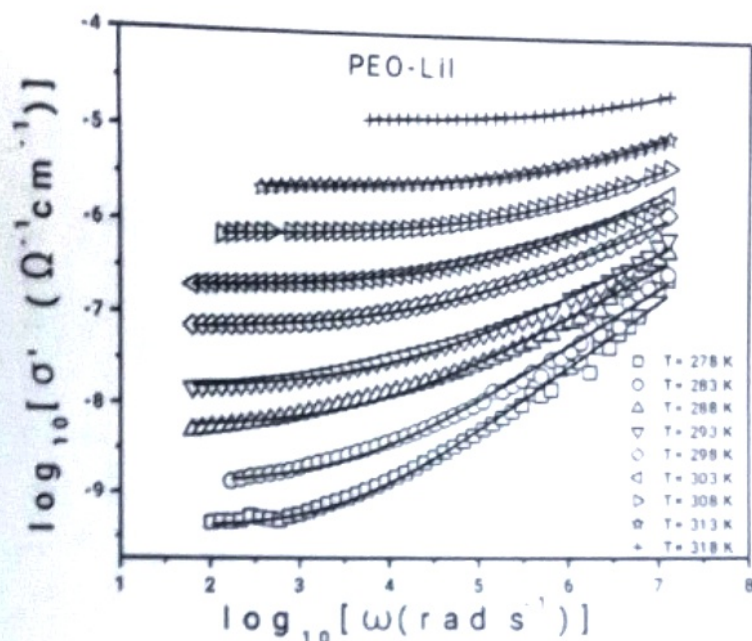


Fig 3.7: Log( $\sigma$ ) vs. Log( $\omega$ ) plot, at different temperatures (278K – 318 K) for PEO-LiI electrolyte

This high probability is responsible for the higher conductivity in higher frequencies and shows dispersion. It is observed from Fig. 3.7 and Fig 3.8 that as the temperature is increased the dc conductivity increases and the switch over from the frequency independent to the frequency dependent region, which marks the onset of conductivity relaxation, shifts towards higher frequencies. From Fig. 3.9 it is observed that at T=293 K the dc conductivity is much higher for ZnO doped PEO-LiI nanocomposite electrolyte. Thus the addition of ZnO nanoparticles into polymer electrolytes is an effective to increase the dc conductivity of the sample.

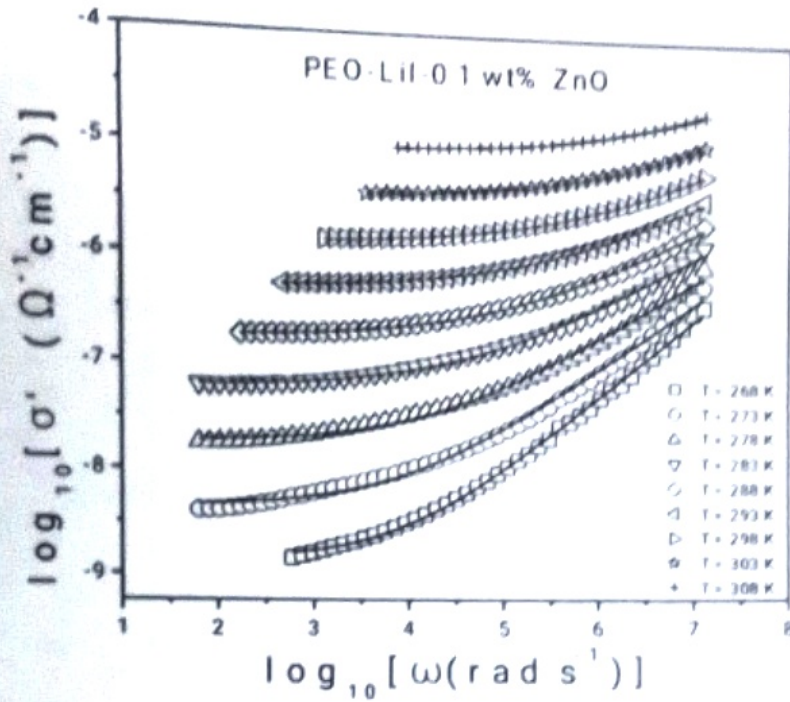


Fig 3.8: Log ( $\sigma$ ) vs. Log ( $\omega$ ) plot, at different temperatures (268K – 308K) for PEO-LiI-0.1 wt% ZnO electrolyte

The dynamics of the  $\text{Li}^+$  ions in the polymer matrix has been studied in the framework of in the framework of the power law formalisms<sup>23,25</sup>. In this formalism the ac conductivity  $\sigma'(\omega)$  is expressed by

$$\sigma'(\omega) = \sigma_{dc} \left[ 1 + \left( \frac{\omega}{\omega_c} \right)^n \right] \quad (6)$$

where  $\omega_c$  is the crossover frequency of the charge carriers and  $n$  is the frequency exponent in the range  $0 < n < 1$ . We have applied the above model to study the ac conductivity of the materials under investigation. The conductivity data at different temperatures have been fitted to Eq. 6, using  $\sigma_{dc}$ ,  $\omega_c$  and  $n$  as variable parameters, using

Microcal Origin 6.0 software. The solid lines in Fig. 3.7 and Fig. 3.8 show such type of fitting. The dc conductivity obtained from the above fitting has been shown in Fig. 3.10.

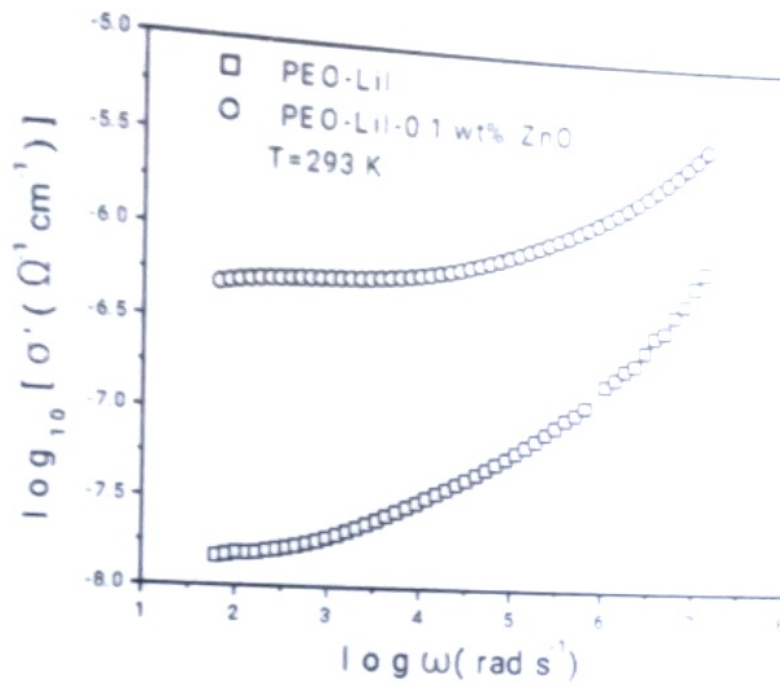


Fig 3.9: Ac conductivity spectra at T=293 K shown as a function of frequency for PEO-LiI and PEO-LiI-0.1 wt% ZnO polymer electrolytes

We have observed that the values of  $\sigma_{dc}$  obtained from the fits match perfectly with those obtained from complex impedance plot (Fig. 3.6) and a close match of the  $\epsilon_s$  value is found. It is observed that for all temperatures the dc conductivity of PEO-LiI-0.1 wt% ZnO polymer nanocomposite electrolytes is higher than PEO-LiI polymer electrolytes. At lower temperatures the difference is higher and at higher temperature i.e. close to melting temperature the difference is small, actually they tends to meet with each other.

The variation of the crossover frequency, obtained from the fit, with reciprocal

temperature is shown in Fig. 3.11. It is noted that crossover frequency is thermally activated. The activation energy  $E_c$  for the crossover frequency was obtained from least square straight line fits of the data and is shown in the graph. It is observed that these activation energies are in good agreement with those for the dc conductivity. It is further noted that the value of  $\omega_c$  is higher for the composites for which the value of the dc conductivity is higher. The above results suggest that the hopping process with same barrier energy is responsible for the dc conduction and ac relaxation. From the above results it can be concluded that the dc conductivity of all the electrolytes occur due to the hopping of charge carriers within the PEO matrix. It is well known that the hopping rate is correlated with the mobility ( $\mu$ )<sup>26</sup>.

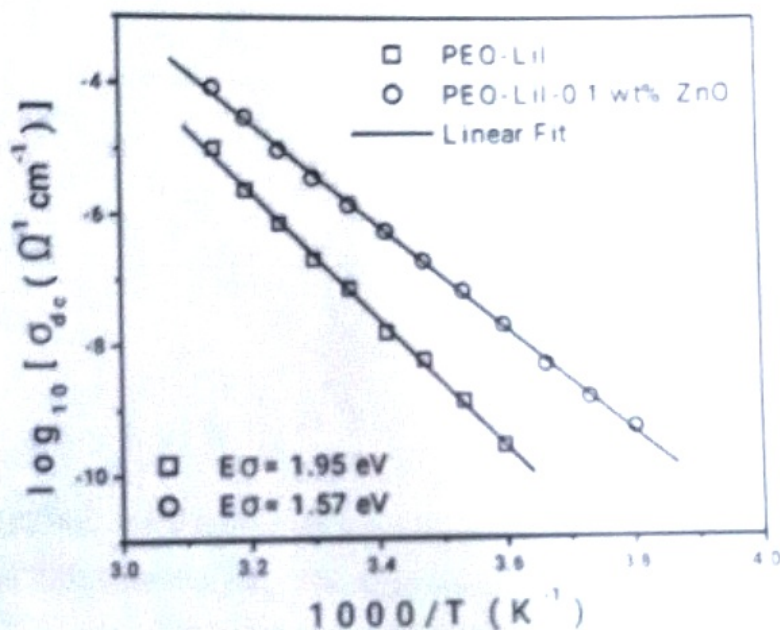


Fig. 3.10: Dc conductivity plotted as a function of inverse temperature for PEO-LiI and PEO-LiI-0.1 wt% ZnO electrolytes. The solid lines are the least square straight-line fits to the experimental data.

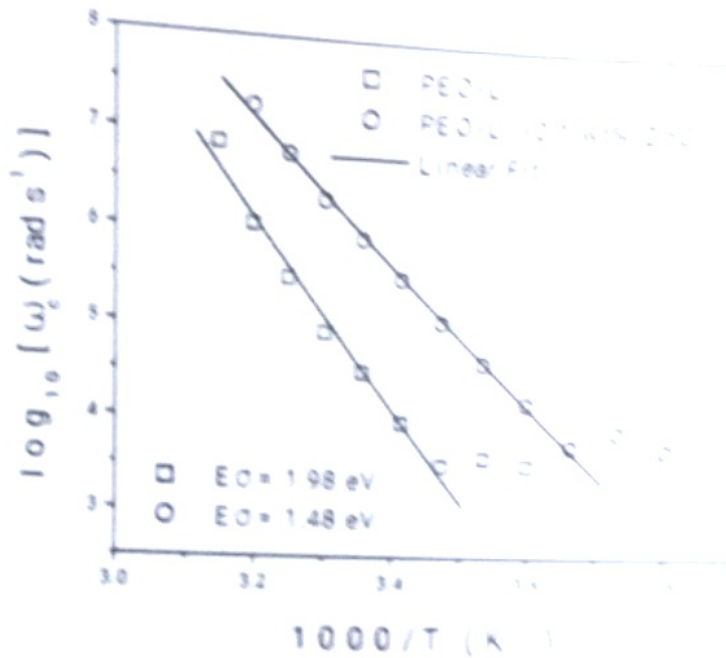


Fig. 3.11: Crossover frequency plotted as a function of inverse temperature for PEO-LiI and PEO-LiI-0.1 wt% ZnO electrolytes. The solid lines are the least square straight line fits to the experimental data

Higher is the hopping rate, higher is the mobility ( $\mu$ ) and thus higher is the conductivity. This hopping rate of charge carriers in the PEO matrix plays an important role for increasing the conductivity level.

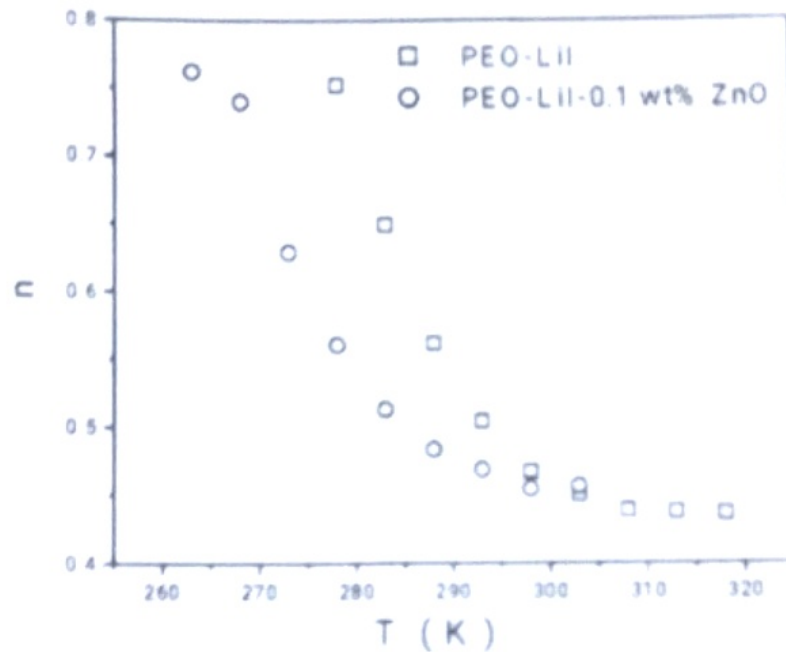


Fig. 3.12: Dependence of frequency exponent on temperature for PEO-LiI and PEO LiI 0.1 wt% ZnO polymer electrolytes

Temperature dependence of the parameter  $n$  provides some information about the interaction between the mobile charge carriers. In general, the value of  $n$  is less than unity. However, the values of  $n$  greater than unity have been observed for some polymeric materials<sup>27</sup>. In some glassy and ceramic materials the value of  $n$  is found to be independent of temperature. But there are some reports on ceramic and glassy systems<sup>28-31</sup> where the value of  $n$  decreases with the increase of temperature, due to the interaction between the mobile ions available in the matrix. The value of  $n$  obtained from curve fitting analysis to the ac conductivity spectra using eq. 3 gets affected by the "window effect". Jain et. al.<sup>32</sup> and Sidebottom<sup>33</sup> have shown that when one truncates

the higher frequency data from the spectra during the fitting procedure the value of  $n$  increases. For obtaining a meaningful exponent only those data sets have to consider for which  $\omega_{\max}/\omega_c > 10$  (in our study  $\omega_{\max} = 2\pi f_{\max}$ , where  $f_{\max} = 2\text{MHz}$ ) and in that case the "window effect" is negligible. Here we have taken only those values of  $n$  for which  $\omega_{\max}/\omega_c > 10$  and the variation of  $n$  with temperature have been displayed in Fig. 3.12 for the PEO-LiI and PEO-LiI-0.1 wt % ZnO nanocomposite electrolytes. It is noted that at low temperatures the parameter  $n$  has a high value and with the increase of temperature the value of  $n$  decreases and attains nearly a constant value. The decrease of  $n$  with the increase of temperature suggests weaker correlation effects among lithium ions<sup>34</sup>

#### 4. CONCLUSION:

In this study, the experimental data of PEO-LiI and novel PEO-LiI polymer nanocomposite electrolyte embedded with ZnO nanoparticles with improved electrical conductivity has been analyzed. The addition of 0.1 wt% ZnO into the PEO-LiI matrix, increases the amorphous phase of PEO and also lowers the melting temperature and glass transition temperature. At this doping level the nanocomposite electrolyte forms a good complexion and a significant enhancement of the dc conductivity has been observed. The temperature dependence of the dc conductivity of the ZnO-doped electrolytes is well explained by the Arrhenius relation. The values of  $\sigma_{dc}$  obtained from ac conductivity spectra match perfectly with those obtained from complex impedance plot and a close match of the  $E_a$  value is found. The activation energy  $E_a$  for the crossover frequency are in good agreement with those for the dc conductivity. With the increase of temperature the frequency exponent  $n$  is found to decrease which suggest a weaker correlation effects among lithium ions.

# BIBLIOGRAPHY

- Practical Guidelines of fluid therapy ,Dr. Sanjay Panday
- Fluid Electrlytes and Acid-Base , Gireesh Kumar K.P
- Refresher course in Physics (Vol- II & III), C.L.Arora
- YouTube channel – Qamarwali\_Ph.D.



**ACKNOWLEDGEMENT** : I would like to acknowledge and give my warm thanks to my teachers and my guide Mr. Suman Mondal under whose supervision I have been able to complete my dissertation

I would like to thank my committee members for letting my defense be an enjoyable moment. I am also grateful to my classmates for their help in editing, late – night feedback and immense mental support which impacted and inspired me in every stage of this journey

Thank You

